Catal Lett (2008) 122:106–110
DOI 10.1007/s10562-007-9350-z

Sulfated TiO_2 Decontaminate 2-CEES and DMMP in Vapor Phase

ShiTong Han · GuoYing Zhang · HaiLing Xi · DaNian Xu · XianZhi Fu · XuXu Wang

Received: 9 September 2007 / Accepted: 7 November 2007 / Published online: 4 December 2007

Abstract An acid photocatalyst TiO_2, modified with H_2SO_4, is prepared and used to decontaminate Chemical Warfare Agents (CWAs) simulants 2-CEES (2-chloroethyl ethyl sulfide) and DMMP (dimethyl methylphosphonate) in vapor phase. Compared with the unmodified pure TiO_2 photocatalyst, the adsorption capacity on the sulfated photocatalyst increases by 50%, and the conversion for 2-CEES increases more than 20%. It is found that the durability for decontaminating DMMP is delayed by 200 min with the modified photocatalyst. The surface characteristics of the photocatalysts are analyzed by XPS and FT-IR. The results show that more Lewis and Brönsted acid sites, considered to be responsible for improving the reactivity performance of photocatalysts, are formed on the sulfated TiO_2.

Keywords Photocatalysis · Decontamination · Sulfated TiO_2 · DMMP · 2-CEES

1 Introduction

Conventional methods for purification of Chemical Warfare Agents (CWAs) polluted air, such as, activated carbon adsorption, incineration and chemical neutralization, are not efficient and create serious post-pollution [1]. Photocatalysis approach, as a new developing and advanced oxidation technology, has been widely applied to the environmental purification [2]. Depended on considerable investigations, researchers have found that photocatalysis method is also effective to decontaminate CWAs and simulants [3–17]. Vorontsov et al. [5–7] investigated the decontamination of Mustard gas simulant 2-CEES over different TiO_2, and found the main products in the gas phase were CH_3CHO, CH_3COOH, C_2H_4, CO_2, H_2O, HCl, and the surface products were CH_3COOH, disulfide, sulfoxide (trace), sulfone, SO_4^{2-}, etc. Hoffman [11] studied the photooxidation of gaseous Sarin simulant DMMP on TiO_2. The main vapor products, including CH_3OH, HCHO, HCOOH, CO_2, H_2O, and the main surface products, including MMP (methyl methylphosphonate), MPA (methylphosphonate acid), HCOOH and PO_4^{-3}, were detected. The results of these researches indicate that 2-CEES and DMMP could be effectively decomposed by photocatalysts. However, most of above mentioned surface products could be deposited on the surface of photocatalysts and lead to the catalyst deactivation. It is reported lately that both high surface area of TiO_2 and appropriate humidity can improve the performance of photocatalysts [7–11].

Recently, some researchers have investigated the adsorption, decomposition, deactivation of 2-CEES and DMMP on TiO_2 [12–17]. These studies demonstrate that these simulant molecules would be firstly adsorbed on the Lewis acid sites (Ti^{4+}) and the Brönsted acid sites (TiO–H) in surface-bound form. Sulfur atom in 2-CEES and phosphorus atom in DMMP, which can act as Lewis bases, would donate a lone pair of electrons to the Lewis acid, or bond with the isolated hydroxyl groups. And then, the active species, such as, O^{2-},·OH, created over TiO_2 on UV radiation, would react with those chemisorption compounds [14–17]. In fact, toluene, benzene etc, which could also act as Lewis bases, can be decomposed effectively

S. Han (✉) · H. Xi · D. Xu
Research Institute of Chemical Defence, Beijing 102205, China
e-mail: honstrong@hotmail.com

S. Han · G. Zhang · X. Fu · X. Wang
Research Institutes of Photocatalysis, Fuzhou University, Fuzhou, Fujian 350002, China

over sulfated TiO_2 [18–20]. So it is deduced that 2-CEES and DMMP are most likely to be adsorbed onto the sulfated TiO_2 surface by means of strong interactions with the surface and would be decomposed effectively.

In this work, a sulfated TiO_2 is prepared and the physical and chemical properties of different TiO_2 are charactered. The adsorption amounts of 2-CEES and DMMP on the sulfated TiO_2 and pure one are investigated and compared. The photocatalytic decomposition of 2-CEES and DMMP are also investigated, and the main intermediate and final products are detected. The main reasons for the improvement of the performance of the sulfated TiO_2 are discussed.

2 Experimental

The ST200 photocatalyst is prepared by reacting amorphous TiO_2 [18, 19] with H_2SO_4 (1 g TiO_2:1 mL H_2SO_4 (1 mol/L)) and drying at 80 °C for 6 h, and then sintered at 200 °C (ST200) for 3 h, the pure TiO_2 is also prepared at the same condition, just without H_2SO_4 (T200).

The photocatalytic reactivity measurement is carried out in a fixed-bed reactor, operated at atmospheric pressure. A quartz tube (outside diameter = 4 mm, inner diameter = 2.8 nm), surrounded by 4 fluorescence lamps (Philips, TUV 4W/G4 T5) with max emission wavelength of 254 nm, is located at the centre of the reactor. 0.1 g catalyst is placed in the centre of the tube. The complete description of the reactor and its operation is presented elsewhere [19, 21].

DMMP (Fluka, 99%) and 2-CEES (Aldrich, 98%) are generated by vaporizing those in a temperature-controlled-water bath and combined with zero air [7–11]. The initial concentrations of 2-CEES and DMMP are 85 and 210 ppm, respectively.

The gas flow rate is 20 cm^3/min in all experiments and analyzed by an online GC (Agilent 6890N) and GC/MS (HP 6890 GC/5972 MSD), with a HP-5 column (0.25 mm × 0.1 μm × 30 m). GC is equipped with a flame ionization detector, a thermal conductivity detector, and a Porapak R column, and is calibrated for CO_2, 2-CEES, DMMP, C_2H_4, HCHO, CH_3OH, and CH_3CHO. We use derivatization techniques to analyze the unknown nonvolatile products qualitatively. Bis (trimethylsilyl) trifluoroacetamide +1% trimethylchlorosilane (BSTFA + 1%TMCS) is used as the derivatization reagent and is purchased from Supelco [4–10].

The temperature of reactions was controlled at 63 ± 2 °C for 2-CEES and 73 ± 2 °C for DMMP. The gas line is kept at 65–75 °C with the help of heating tapes in order to avoid condensation and adsorption of reactants and products.

Prior to the adsorption, the catalyst is dried at 110 °C over night, then, it is placed in the tube immediately. The adsorption reaction carries out at room temperature. The detail experimental process of 2-CEES and DMMP is described in Sects. 3.2 and 3.3.

IR spectra of the samples (ca.15 mg/cm^2), pressed into a self-supporting thin wafer, are recorded on a Nicolet 670 FT-IR spectrometer at a resolution of 4 cm^{-1}. The nitrogen adsorption–desorption isotherms of samples (vacuum-dried at 120 °C overnight) at 77 K are measured with an Omnisorp 100CX system. X-ray diffraction (XRD) measurements are performed on a Bruker D8 Advance X-ray diffractometer with Cu Kα radiation. The crystal size is calculated from the full width at half maximum of anatase (101) by Sherrer equation. X-ray photoelectron spectra (XPS) of the samples are recorded on a Quantum 2000 spectrometer with mono-chromatised Al Kα X-rays (hν = 1486.6 eV) operating at 150 W. The sample, which is pressed into a sheet and sealed in glass tube, is transferred and enclosed in a stub with conductive carbon tape in a glove box. The core-level binding energies (BE) are referenced to the C1s line at 284.5 eV. The spectra are fitted by XPS Peak Fitting Program (Version 4.1) with a constant or chosen half-maximum (FWHM) of the peaks.

Because the CWAs are very hazardous and not suitable to research in laboratory [1], 2-CEES, the stimulant of Mustard and DMMP, the stimulant of Sarin, are chosen as the reactants here. Due to their structure, the simulants are expected to be less reactive than CWAs, and provide a conservative estimate for the potential of TiO_2 photocatalysis for the decontamination of hazardous organophosphorous and organosulfur compounds [3–17].

3 Results and Discussions

3.1 The Physical and Chemical Properties of the Sulfated TiO_2 (ST200) and Pure TiO_2 (T200)

3.1.1 Surface Areas and Crystal Sizes of ST200 and T200

The results of our previous work confirmed that the photocatalyst would behave with the best performance, when calcined at 200 °C for 3 h [21]. Table 1 shows the specific surface areas and crystal sizes of ST200 and T200. As shown in Table 1, the specific surface areas and the anatase crystal sizes of ST200 and T200 are almost the same.

3.1.2 IR Spectra of ST200 and T200

The IR spectra of ST200 and T200, shown in Fig. 1, are distinct. The sharp peaks of ST200, observed at 1,219,

Table 1 Physical and chemical properties of different samples

	T200	ST200	P25
Crystal structure[a]	100%A	100%A	70%A, 30%R
Crystal size (nm)	6	5	30
Surface area (BET) (m^2/g)	216	221	50

[a] A: Anatase, R: Rutile

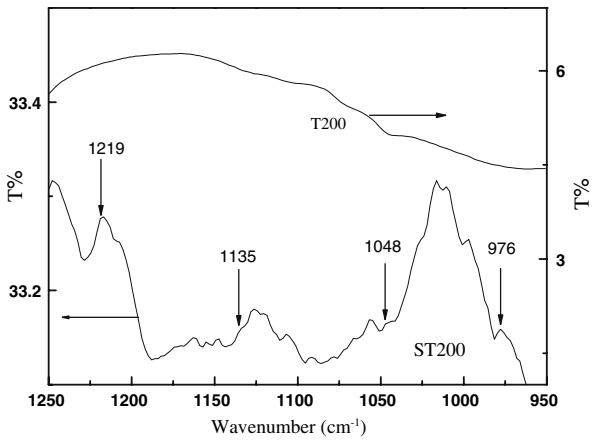

Fig. 1 FT-IR spectra of T200 and ST200 catalysts

1,135, 1,048, and 976 cm^{-1} [19], are assigned to a bidentate SO_4^{2-} coordinated to metals, such as Ti^{4+}. The peak at about 1,020 cm^{-1} has the highest intensity and may be attributed to bidentately bound sulfate ion [22]. The bridge bidentate structure could withdraw electrons from the neighboring Ti cations strongly, indicating a very strong interaction between the sulfate anion and titanium cation, which is believed to be a driving force in the generation of a large amount of surface acidic sites on photocatalyst [19]. However, the IR spectra of T200 is simple and without these peaks.

3.1.3 The XPS Spectra of ST200 and T200

The curve-fitting results of the XPS spectra of O2p on ST200 and T200 are shown in Fig. 2. Two dominant peaks about 529.7 and 531.4 eV, related with lattice oxygen, surface hydroxyl oxygen respectively, are presented on T200. However, there are three dominant peaks on ST200, they are 530.20 eV (lattice oxygen), 531.89 eV (surface hydroxyl oxygen) and 530.73 eV (oxygen in sulfate species), respectively [20, 23–25]. It is believed that the peak about 530.7 eV is attributed to the effects of SO_4^{2-} on TiO_2 and this result is consistent with the results of IR spectra. The slight increase of BE suggests that SO_4^{2-} would change the electronegativity of O atoms.

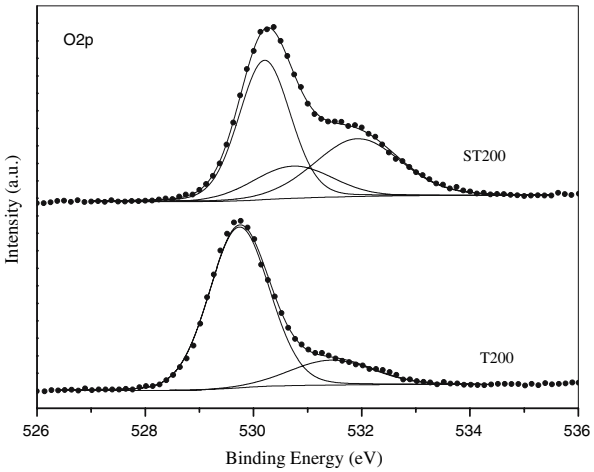

Fig. 2 XPS spectra of the O2p region for ST200 and T200

Table 2 Curve-fitting result of O2p region over T200 and ST200

	Lattice oxygen Ti–O	Oxygen in sulfate species S–O	Surface hydroxyl groups Ti–OH
T200	529.74 eV	–	531.44 eV
	83.05%	–	16.95%
ST200	530.20 eV	530.73 eV	531.89 eV
	49.64%	16.41%	33.95%

Table 2 lists the results of curve fitting of O2p XPS spectra. It is found that the area of O2p increases obviously after sulfation, and the amount of the surface hydroxyl oxygen of ST200 is about two times of that of T200, which was also found in our previous work [19].

3.2 Photocatalytic Decomposition of 2-CEES Over Different Photocatalysts

Initial blank experiments show that both UV light and TiO_2 are necessary to oxide 2-CEES [5–7]. Additionally, prior to starting the photocatalytic experiments, 2-CEES molecules are adsorbed into the catalysts until the concentrations of outlet flow is equal to that of inlet flow.

The 2-CEES conversion (define as one minus the ratio of concentration of 2-CEES in the effluent stream to the concentration of 2-CEES in the inlet stream) over different TiO_2 photocatalysts after switching on the lamps is illustrated in Fig. 3. The initial conversion is below zero (not shown in Fig. 3), the reason is that 2-CEES concentration of outlet exceeds that of inlet just in the start of irradiation due to desorption. Then, 2-CEES concentration falls well below that of inlet. Subsequently, 2-CEES concentration would gradually increase with time, which is a sign of

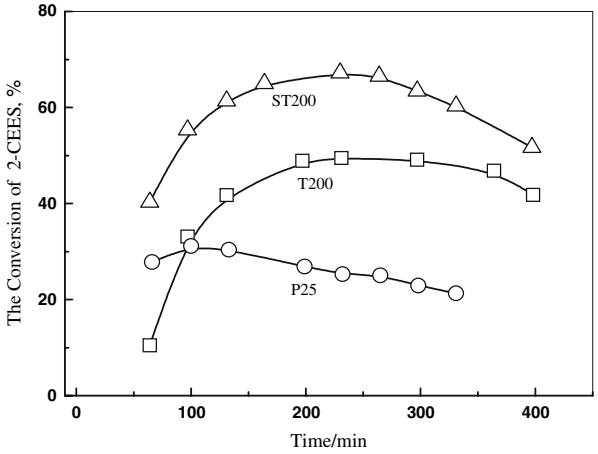

Fig. 3 Photocatalytic conversion of 2-CEES over different catalysts. $C_{2\text{-CEES}}$ = 85 ± 5 ppm, T = 63 ± 2 °C, flow rate 20 cm^3/min, relative humidity <1%

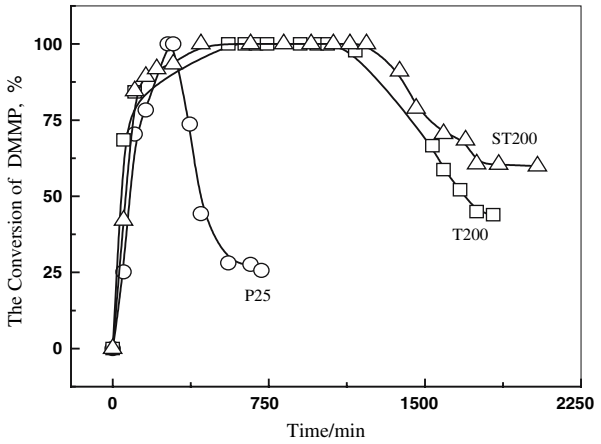

Fig. 4 Photocatalytic conversion of DMMP over different catalysts. C_{DMMP} = 210 ± 10 ppm, T = 73 ± 2 °C, flow rate 20 cm^3/min, relative humidity <1%

catalyst deactivation. The main gas phase products, including CO_2, C_2H_4, CH_3CHO, $C_2H_5SC_2H_5$, $C_2H_5S_2C_2H_5$, are detected over all these three photocatalysts, and the main surface products, mainly including, $C_2H_5S_2C_2H_5$, $C_2H_5SC_2H_4OH$, $C_4H_9S_2C_2H_5$, $C_2H_5S_2C_2H_4OH$, are also detected. The similar surface products were detected on P25, Hombikat UV 100 TiO_2 and other types TiO_2 in works [5–7, 16, 17]. So, it is suggested that the reaction routes on ST200 are similar to that on P25 and T200. Amounts of intermediate products are accumulated on the catalyst surface, causing the reduction of the adsorption plenty of oxygen, which would improve the recombination of h^+ and e^- [26]. Furthermore, these intermediate products would occupy the adsorptive site of the catalysts, blocking the adsorption amount of objects [27]. These results may be the reason for the catalysts deactivation.

It could also be seen in Fig. 3, that the highest conversion of 2-CEES is gained over ST200 among these three photocatalysts, while, P25 is most liable to deactivate. The conversion of 2-CEES over ST200 exceeds 50% till 400 min for photocatalytic reaction, which is about two times of that over P25 in the whole range of time. Moreover, compared with T200, an increase of the conversion of 2-CEES by more than 20% is obtained over ST200.

3.3 Photocatalystic Decomposition of DMMP Over Different Photocatalysts

The reaction of DMMP is obviously different from that of 2-CEES. The decomposition reaction of DMMP would occur as long as DMMP molecules are adsorbed on the catalyst [10–13]. So, the photocatalytic reaction starts once the gas flow gets through the reactor.

The conversion of DMMP over catalysts is shown in Fig. 4. It takes about 120 min for the conversion to reach 100%, after the lamp opens. During this period, the adsorption, hydrolysis and photocatalysis reaction occurs simultaneously [12, 13]. The conversion keeps 100% for a long time. And then, it begins to fall, indicating that the decontamination reaction slows down and the catalyst deactivates.

It is also shown in Fig. 4 that ST200 has the best reactivity among three photocatalysts, and it is steadier than T200, because the conversion can keep 100% for 1,300 min over ST200, however, it is just about 1,000 min over T200. P25 is easy to deactivate, because the conversion of DMMP over P25 starts to decrease just at 420 min and drops from 100% to 30% in 200 min.

The volatile products are mainly CO_2, CH_3OH, HCOOH, HCHO and non-volatile surface product is MPA (methyl methylphosphonic acid) [10–13]. The compounds, containing P atoms, could not be found in gas. So, it is suggested that all P atoms be deposited on TiO_2 surface, leading to the catalyst deactivation.

3.4 The Adsorption Quantities of 2-CEES and DMMP on the Surface of Different TiO_2 Photocatalysts

Table 3 shows the adsorption quantities of 2-CEES and DMMMP on ST200, T200 and P25, respectively. As seen in Table 3, ST200 improves strongly the adsorption capacity. Compared with T200, the adsorption quantity of 2-CEES increases by 60% over ST200, and just about 4.98 μL of 2-CEES is adsorbed on P25, which is less than one third of that on ST200. The adsorption and reactivity amount of DMMP is about 326 μL over ST200, which is

Table 3 Cumulative consumption amounts of 2-CEES, DMMP in adsorption processes (μL) $C_{2\text{-CEES}} = 85 \pm 5$ ppm, $C_{DMMP} = 210 \pm 10$ ppm, flow rate 20 cm^3/min, relative humidity <1%, room temperature

	ST200	T200	P25
2-CEES	14	8.51	4.98
DMMP[a]	326	283	69

[a] The amount of adsorption and reactivity

close to 5 times of P25, while, the adsorption amount over T200 is about 4 times of P25.

The first main reason for the above results is that a large number of acid sites can be formed on the sulfated TiO_2 [18–20]. An anatase surface has two main types of active sites: exposed cation Ti surface site and Ti–OH with characters of Lewis acid and Brönsted acid, respectively [23]. Yates has demonstrated that 2-CEES molecule can bind to Ti–OH groups via both chlorine and sulfur atoms [14–17], and –P=O in DMMP could coordinate with the two above-mentioned acid sites [12, 13]. The result of IR spectra in the Sect. 1.2 also indicates that much more Lewis acid and Brönsted acid sits are formed on ST200. Additionally, surface hydroxyl oxygen of ST200 is more than two times of that of T200, which accounts for the production of much more Ti–OH sites on the surface of ST200. The experimental data imply the improvement of the adsorption capacity of ST200.

The other main reason for the above results is that surface hydroxyl plays a very important role in photocatalysis, because the surface hydroxyl would scavenge the photoexcited holes from the valence band of TiO_2 and would form some active species, such as ·OH, and these processes are rate-determining steps of photocatalysis [3, 19]. The results of XPS spectra present that much more surface hydrolysis are formed on ST200. So, the acid photocatalysts would behave with a better performance for 2-CEES and DMMP.

Finally, the main intermediates—partial oxidation products deposited on surface are found to be surface bound formate-carboxylate-carbon (R–COO–), phosphate(R–POO–) and sulfate (R–SOO–) etc. [12–17, 23], which would block absorption of O_2, but also would prevent the formation of active species. Although it is mentioned above that the main intermediate products may be unchanged on these catalysts, and the reaction routes on ST200 are similar to that on P25 and T200, the durability and reaction activity of ST200 is better than the others. So, the formation amounts of these intermediate products on ST200 is much smaller than these on T200 and P25 during the reaction process, implying that the sulfated TiO_2 reduce the quantity of these unwanted intermediates, and thus improve the stability of photocatalysts.

In conclusion, the results of XPS and FT-IR show much more acid sites and surface hydroxyl are formed on the sulfated TiO_2, causing higher adsorption capacity and reactivity over the sulfated TiO_2 than over the pure TiO_2.

Acknowledgments The work described here is financially supported by the National Natural Science Foundation of China (Nos. 20473113).

References

1. Yang Y-C, Baker JA, Ward JR (1992) Chem Rev 92:1729
2. Hoffman MR, Matin ST, Choi W et al (1995) Chem Rev 95:69
3. Fox MA, Kim YS, Abdel-Wahab AA et al (1990) Catal Lett 5:369
4. Obee TN, Satyapal S (1990) J Photochem Photobiol A: Chem 118:45
5. Vorontsov AV, Savinov EN, Davydov L (2001) Appl Catal B: Environ 32:11
6. Vorontsov AV, Panchenko AA, Savinov EN et al (2002) J Environ Sci Technol 36:5261
7. Vorontsov AV, Lion C, Savinov EN et al (2003) J Catal 220:414
8. Vorontsov AV, Savinov EN, Davydov L (2003) Appl Catal B: Environ 44:25
9. Mrtyanov I, Klabunde KJ (2003) J Environ Sci Technol 37:3448
10. Trubitsyn DA, Vorontsov AV (2005) J Phys Chem B 109:21884
11. Moss JA, Szczepankiewicz SH, Hoffman MR et al (2005) J Phys Chem B 109:19779
12. Rusu CN, Yates JT Jr (2000) J Phys Chem B 104:12292
13. Rusu CN, Yates JT Jr (2000) J Phys Chem B 104:12299
14. Panayotov DA, Yates JT Jr (2003) J Phys Chem B 107:10560
15. Panayotov DA, Yates JT Jr (2004) Langmuir 20:3674
16. Thompson TL, Panayotov DA, Yates JT Jr (2004) J Phys Chem B 108:16825
17. Thompson TL, Panayotov DA, Yates JT Jr (2004) J Phys Chem B 108:17857
18. Fu XZ, Zeltner WA, Yang Q et al (1997) J Catal 168:2
19. Wang XC, Yu JC, Liu P, Wang X et al (2006) J Photochem Photobiol A: Chem 179:339
20. Barraud E, Bosc F, Edwards D et al (2005) J Catal 235:318
21. Han ST, Xi HL, Fu XZ et al (2005) Chin J Environ Sci 26:130
22. Samantaray SK, Mishra T, Parida KM (2000) J Mol Catal A: Chem 156:267
23. Kiselev A, Mattson A, Andersson M et al (2006) J Photochem Photobio A: Chem 184:125
24. Colón G, Hidalgo MC, Munuera G et al (2005) Appl Catal B: Environ 63:45
25. Yang QJ, Xie C, Xu ZL et al (2006) J Phys Chem B 110:7
26. Kim SB, Hwang HT, Hong SC (2002) Chemosphere 48:437
27. Méndenz-Román R, Cardona-Martínez N (1998) Catal Today 40:353